

# Process optimization and characterization of activated carbons from *Amygdalus pedunculata* shell by zinc chloride activation

Y. SHU, C. LI, B. CHEN, W. BAI, Y. SHEN\*

Key Laboratory of Synthetic and Natural Functional Molecule Chemistry of Ministry of Education / College of Chemistry and Materials Science, Shaanxi Alcohol Ether and Biomass Energy Engineering Research Center / Key laboratory of Yulin Desert Plants Resources, Northwest University, 229 Taibai North Road, Xi'an 710069, China

The use of high carbonous, huge amount and low-cost agricultural wastes as feedstock for production of activated carbon is an effective means for reducing environmental pollution and increasing economic benefits. In this work, Activated carbons were produced from *Amygdalus pedunculata* shell with zinc chloride as activating agent using Box-Behnken design. The effects of process variables (concentration of zinc chloride, activation time, and activation temperature) on textural and chemical-surface properties of activated carbon were studied. The yield and adsorption capacity (iodine and methylene blue) of activated carbons were evaluated by three quadratic models, analysis of variance, and three-dimensional surface plots using Design-Expert software. The predicted results by the models were found to be in good agreement with the experimental results for activated carbons prepared in the optimum conditions as follows: yield (48.8%), iodine value (1448 mg/g), and methylene blue value (280 mg/g). The activated carbons obtained under the best conditions were characterized using N<sub>2</sub> adsorption/desorption isotherms, X-ray diffraction (XRD), scanning electron microscopy (SEM) and Fourier transform infrared spectroscopy (FT-IR).

(Received July 15, 2014; accepted January 21, 2015)

**Keywords:** *Amygdalus pedunculata* shell, Activated carbon, Zinc chloride, Box-Behnken design

## 1. Introduction

Because of their large surface area and high degree of surface reactivity, activated carbons are widely used in chemical, pharmaceutical, and food industries [1,2]. Typical precursors for activated carbons are coal, wood, and coconut shells [3-5]. Recently, agricultural and forest wastes are being considered as important feedstock for activated carbon preparation because they are renewable, available in huge amounts, and less costly [6-8]. A number of raw lignocellulosic materials such as olive stones [9], peanut hulls [10], acorn shell [11], date stones [12,13], and wood sawdust [14] have been utilized for the preparation of activated carbons with high adsorption capacity.

*Amygdalus pedunculata* Pall. (*A. pedunculata*), a member of the family Rosaceae, is a type of sand dune-stabilizing and oil-bearing shrubs. It mainly grows in the arid regions of northwestern China and Mongolia. Their high tolerance to cold and drought stresses, deep root system, and greater adaptability to a wide range of soil types and soil moisture conditions make them as a good candidate for desert reclamation [15]. *A. pedunculata* kernel contains 40–50% fat, 20–30% protein, and 3% amygdalin. It could be used to prepared edible oil [16], biodiesel [15], and protein. *A. pedunculata* possesses

significant economic and ecological protection value. The State Forestry Administration of the People's Republic of China has approved a planting scheme for one million acres of *Amygdalus pedunculata* and 300,000 acres have already been cultivated with this plant in Yulin, China. The fruit yield is ~6,000 kg/ha per year at peak time with the fruit containing 70–80% *A. pedunculata* shell by weight. The *A. pedunculata* shells are rich in carbon and possess significant mechanical strength and low ash content besides being abundant in nature and less-costly, and therefore, they can be utilized in the production of activated carbons [17].

Activated carbons are prepared through physical [18,19] or chemical activation [20-22]. Compared with physical activation, the results showed that chemical activation produced carbons with higher density and surface areas [23]. The effect of different chemical reagents on the production and quality of activated carbon has been extensively studied [24-27]. In particular, zinc chloride (ZnCl<sub>2</sub>) is widely used in the preparation of activated carbons, as it gives high yield and high adsorption capacity. Response surface methodology (RSM), statistical and mathematical techniques for process optimization, has been successfully applied in studying the production of activated carbons [28-30].

In this study, *A. pedunculata* shells were utilized as feedstock for the preparation of activated carbons by  $\text{ZnCl}_2$  activation. To develop an optimized process for the production of activated carbons with high yield and desired adsorption performances, Box-Behnken design (BBD) [31,32] for RSM was employed. Further, the effects of  $\text{ZnCl}_2$  concentration, activation time, and activation temperature on the yield, and iodine and methylene blue (MB) adsorption values of activated carbons were evaluated. This method is expected to produce activated carbons with higher yield and well-developed porosity from *A. pedunculata* shells, and thereby supply a new feedstock for the activated-carbon industry.

## 2. Materials and methods

### 2.1 Materials

*A. pedunculata* plants were planted in Shenmu county, Yulin, Shaanxi Province, China (geographical coordinates are approximately 38°40' N, 110°08' E) and *A. pedunculata* shells were received from Shenmu County Ecology Protection and Construction Association.

All the chemicals used in this study were of analytical grade and purchased from Tianjin Kemiou Chemical Reagent Co., Ltd., China.

### 2.2 Preparation of activated carbon

The dried precursor (10 g) was added to  $\text{ZnCl}_2$  (40–60 %) solution, and the mixture was allowed to stand for 24 h. Next, the slurries obtained were heated at 105 °C for 2 h. The resulting samples were placed in a muffle furnace and heated to 300 °C for 1h. The samples were then chemically activated at different activation temperatures (500–700 °C) and activation time (90–150 min). After the activation process, the samples were cooled down to room temperature. The samples were then washed sequentially with 1.0 mol/L HCl, hot water, and finally distilled water to remove the residual organic and mineral substances until the pH of the washing solution become neutral, and then dried at 105°C. Finally, the dried samples were crushed and sieved through a 200 mesh and stored in tightly closed bottles.

### 2.3 Multivariate experimental design

A standard RSM design, BBD, was used to study the process variables for the preparation of activated carbons from *A. pedunculata* shells.

Based on preliminary studies and the results of single-factor experiments, concentration of  $\text{ZnCl}_2$  ( $X_1$ ), activation time ( $X_2$ ), and activation temperature ( $X_3$ ) were selected as three important independent process variables. The dependent process variables were the activated carbon yield ( $Y_1$ ), iodine adsorption value ( $Y_2$ ), and MB adsorption value ( $Y_3$ ). A 3-factor, 3-level and 17-run BBD

method was applied to statistically optimize the preparation of activated carbons from *A. pedunculata* shell. The selection range of respective process variables, coded as -1, 0 and +1, is given in Table 1.

Table 1. Independent variables their levels used for BBD.

Level	Variables		
	$X_1$ Concentration of $\text{ZnCl}_2$ / %	$X_2$ Activation time / min	$X_3$ Activation temperature / °C
-1	40	90	500
0	50	120	600
1	60	150	700

The three test process variables were coded according to the following equation:

$$x_i = (X_i - X_0) / \Delta X \quad i = 1, 2, 3 \quad (1)$$

where,  $x_i$  and  $X_i$  are the coded value and the actual value of independent variable, respectively,  $X_0$  is the actual value of the independent variable at the center point, and  $\Delta X$  is the step-change value of the independent variable. A second-order model was fitted to correlate the relationship between the independent variable and the responses (yield, iodine value, and MB value) in order to predict the optimum conditions.

$$Y = A_0 + \sum_{i=1}^3 A_i X_i + \sum_{i=1}^3 A_{ii} X_i^2 + \sum_{i=1}^2 \sum_{j=i+1}^3 A_{ij} X_i X_j \quad (2)$$

where,  $Y$  is the dependent variable (yield, iodine value or MB value),  $A_0$  is a constant, and  $A_i$ ,  $A_{ii}$ ,  $A_{ij}$  are the coefficients calculated by using the model.  $X_i$  and  $X_j$  represent the linear, quadratic and cross-product effects of the  $X_1$ ,  $X_2$ , and  $X_3$  factors on the responses.

### 2.4 Model fitting and statistical analysis

Design-Expert (v.7.1.6, Stat-Ease, Inc., Minneapolis, USA), a statistical software package, was used for the regression analysis of experimental data to fit the equations developed and also to plot three-dimensional response surfaces. Analysis of variance (ANOVA) was used to estimate the statistical parameters. Subsequently, three additional experiments were conducted to validate the statistical experimental strategies.

### 2.5 Process performance

#### 2.5.1 Yield of activated carbons

The yield of activated carbons was calculated by using the following equation:

$$\text{Yield}(\%) = w_c/w_o \times 100 \quad (3)$$

where,  $w_c$  and  $w_o$  are the dry weight (g) of the final activated carbons and dry weight (g) of the precursor (feedstock for activated carbons), respectively.

### 2.5.2 Iodine and methylene blue adsorption

The iodine [33] and MB [34] adsorption properties of the activated carbons were measured according to literatures procedures. Iodine and MB are usually used for the characterization of activated carbon. The iodine value was determined at 298 K based on a Standard Test Method, GB/T 12496.8-1999 (the testing standard for activated carbons in China). The MB adsorption value was determined according to GB/T 12496.10-1999. The iodine and MB values are expressed as milligrams of adsorbate adsorbed onto the surface of 1 g activated carbons.

## 2.6 Characterization of the prepared activated carbon

### 2.6.1 Characterization of pore structure

The pore structure analysis of the prepared activated carbons was performed using a Micromeritics ASAP 2020 Surface Analyzer through nitrogen adsorption at 77 K and  $10^{-6}$ –1 atmospheric pressure. The powder X-ray diffraction (XRD) patterns of the prepared activated carbons were recorded using a Bruker D8 Advance at 40

kV and 40 mA (Cu K  $\alpha$  radiation). The scanning electron microscopy (SEM) analysis of the prepared activated carbons was carried out under optimum conditions using a JEOL JSM-6500F, to observe their surface texture and the development of porosity.

### 2.6.2 Surface chemistry determination

The fourier transform infrared radiation (FTIR) analysis of the prepared activated carbons was conducted to identify the surface functional groups of the precursor and modified carbons using a Bruker TENSOR 27 in 4000–400  $\text{cm}^{-1}$  range.

## 3. Results and discussion

### 3.1 Development of regression model equation

A 17-run BBD with three factors and three levels, including five replicates at the center point, was used to fit a second-order response surface. This was used to study the correlation between the process variables and the yield and iodine/MB adsorption capacity of the prepared activated carbons. The five center-point runs were carried out to measure the process stability and inherent variability. The yield and iodine/MB adsorption capacity of activated carbons were taken as the responses. The results are shown in Table 2 based on the results in Table 1.

Table 2. Box-Behnken experimental design with the independent variables.

Run	Coded level			Yield ( $Y_1$ ), %		Iodine value ( $Y_2$ ), mg/g		MB value ( $Y_3$ ), mg/g	
	$X_1$	$X_2$	$X_3$	Actual	Predicted	Actual	Predicted	Actual	Predicted
1	0	-1	1	36.8	36.7	1437	1465	300	280
2	-1	1	0	48.2	47.8	1455	1435	247	257
3	0	0	0	49.0	48.7	1437	1385	293	293
4	0	1	1	36.2	36.2	1468	1488	263	258
5	0	0	0	49.5	49.2	1533	146	300	280
6	0	0	0	49.2	49.2	1437	1386	293	293
7	1	-1	0	46.1	46.5	1468	1464	237	247
8	0	1	-1	50.9	51.0	1220	1271	217	237
9	0	0	0	48.9	49.2	1437	1462	285	293
10	1	0	1	33.1	32.8	1422	1435	247	237
11	-1	0	1	38.7	39.0	1409	1433	240	255
12	0	-1	-1	51.3	51.3	1409	1433	233	238
13	1	1	0	46.3	46.6	1482	1455	245	240
14	-1	0	-1	48.9	49.2	1380	1349	237	227
15	1	0	-1	52.3	52.0	1395	1371	237	222
16	-1	-1	0	49.0	49.2	1437	1462	250	255
17	0	0	0	49.3	49.2	1468	1462	295	293

The predictive equation was obtained by fitting the experimental data to the BBD model in Eq. (4), (5), and (6), which indicated the relationship between the responses (yield, iodine value, and MB value) and the tested process variables (in coded units) as follows:

$$Y_1 = 49.18 - 0.87X_1 - 0.20X_2 - 7.33X_3 + 0.25X_1X_2 - 2.25X_1X_3 - 0.050X_2X_3 - 1.17X_1^2 - 0.62X_2^2 - 4.76X_3^2 \quad (4)$$

$$Y_2 = 1462.40 + 10.75X_1 - 15.75X_2 + 41.50X_3 - 1.00X_1X_2 - 0.50X_1X_3 + 55.00X_2X_3 + 8.05X_1^2 - 9.95X_2^2 - 68.95X_3^2 \quad (5)$$

$$Y_3 = 293.20 - 1.00X_1 - 6.00X_2 + 15.75X_3 + 2.75X_1X_2 + 1.75X_1X_3 - 5.25X_2X_3 - 30.73X_1^2 - 17.73X_2^2 - 22.22X_3^2 \quad (6)$$

In these equations, positive sign indicates synergistic effect and negative sign indicates antagonistic effect. The response coefficient of the model was estimated by multiple regression analysis technique. The quality of the model was determined from their correlation coefficients.

### 3.2 Statistical analysis

Eq. (2) was used to evaluate the effects of experimental factors on the yield and iodine/MB adsorption of the activated carbons, as shown in Figs. 1, 2, and 3. The credibility of the developed models was evaluated from their correlation coefficients ( $R^2$ ). The proximity of  $R^2$  value to unity and the smaller the standard deviation, indicate the better suitability between the experimental and the predicted values of the model [22]. The  $R^2$  values for Eqs. (4), (5), and (6) are 0.998, 0.738, 0.852, respectively. Further, the standard deviations for Eqs. (4), (5), and (6) are 0.40, 50.18, and 16.26,

respectively. This indicated that the predicted value for  $Y_1$  would be the most accurate and closer to its actual value, compared to  $Y_2$  and  $Y_3$ . The close to unity  $R^2$  values and smaller standard deviations of the model indicate a good agreement between the experimental and predicted values of the model. The accuracy of the models was further justified through analysis of variance (ANOVA). The ANOVA of the quadratic model for the yield of activated carbons is listed in Table 3. The values of model (Prob > F) < 0.0500 indicated that the model terms is significant. Checking the adequacy of model is an important part of the data analysis procedure, because it would result in poor or misleading results if the fit is inadequate [33]. From the ANOVA of activated carbon yield, the value of model (Prob > F) < 0.0001 implied that the model term was very significant. In this case, the concentration of  $ZnCl_2$  ( $X_1$ ), activation time ( $X_2$ ), and the interaction terms ( $X_1X_3$ ,  $X_1^2$ , and  $X_3^2$ ) were found to be significant model terms whereas activation temperature ( $X_3$ ) and the interaction terms ( $X_1X_2$ ,  $X_2^2$ , and  $X_2X_3$ ) were all insignificant to the response. The ANOVA of the quadratic model for iodine/MB adsorption value are listed in Table 4. From the ANOVA of iodine adsorption value, the interaction term ( $X_3^2$ ) was found to be significant whereas other factors were insignificant to the responses. From the ANOVA of MB adsorption value, the model (Prob > F) of 0.0305 implied that the model was significant. In this case, the activation temperature ( $X_3$ ) and the interaction terms ( $X_1^2$  and  $X_3^2$ ) were significant whereas other factors were insignificant to the responses. The statistical results showed that the above models were adequate to predict yield and iodine/MB adsorption capacity of the activated carbons within the range of process variables studied.

Table 3. Analysis of variance (ANOVA) for response surface quadratic model for activated carbon yield ( $Y_1$ ).

Source	Sum of squares	df <sup>a</sup>	Mean square	F-value	Prob > F
Model	564.04	9	62.67	399.54	< 0.0001
$X_1$	6.13	1	6.13	39.05	0.0004
$X_2$	0.32	1	0.32	2.04	0.1963
$X_3$	429.24	1	429.24	2736.53	< 0.0001
$X_1X_2$	0.25	1	0.25	1.59	0.2472
$X_1X_3$	20.25	1	20.25	129.10	< 0.0001
$X_2X_3$	1.000E-002	1	1.000E-002	0.064	0.8079
$X_1^2$	5.71	1	5.71	36.43	0.0005
$X_2^2$	1.59	1	1.59	10.15	0.0154
$X_3^2$	95.60	1	95.60	609.48	< 0.0001
Residual	1.10	7	0.16	-	-
Lack of fit	0.87	3	0.29	5.09	0.0750
Pure error	0.23	4	0.057	-	-
Correlation total	565.14	16	-	-	-

<sup>a</sup> degree of freedom.

Table 4. Analysis of variance (ANOVA) for response surface quadratic model for adsorption of Iodine value ( $Y_2$ ) and methylene blue value ( $Y_3$ ).

Source	Sum of squares		df	Mean square		F-value		Prob > F	
	I <sub>2</sub> ( $Y_2$ )	MB ( $Y_3$ )		I <sub>2</sub> ( $Y_2$ )	MB ( $Y_3$ )	I <sub>2</sub> ( $Y_2$ )	MB ( $Y_3$ )	I <sub>2</sub> ( $Y_2$ )	MB ( $Y_3$ )
Model	49644.74	10617.14	9	5516.08	1179.68	2.19	4.47	0.1569	0.0305
X <sub>1</sub>	924.50	8.00	1	924.50	8.00	0.37	0.030	0.5637	0.8667
X <sub>2</sub>	1984.50	288.00	1	1984.50	288.00	0.79	1.09	0.4041	0.3310
X <sub>3</sub>	13778.00	1984.50	1	13778.00	1984.50	5.47	7.52	0.0519	0.0288
X <sub>1</sub> X <sub>2</sub>	4.00	30.25	1	4.00	30.25	1.589E-003	0.11	0.9693	0.7449
X <sub>1</sub> X <sub>3</sub>	1.00	12.25	1	1.00	12.25	3.971E-004	0.046	0.9847	0.8356
X <sub>2</sub> X <sub>3</sub>	12100.00	110.25	1	121.00	110.25	4.81	0.42	0.0645	0.5387
X <sub>1</sub> <sup>2</sup>	272.85	3974.84	1	272.85	3974.84	0.11	15.06	0.7516	0.0060
X <sub>2</sub> <sup>2</sup>	416.85	1322.84	1	416.85	1322.84	0.17	5.01	0.6963	0.0602
X <sub>3</sub> <sup>2</sup>	20017.27	2079.79	1	200017.27	2079.79	7.95	7.88	0.0258	0.0263
Residual	17626.20	1847.80	7	2518.03	263.97	-	-	-	-
Lack of fit	10675.00	1731.00	3	3558.33	577.00	2.05	19.16	0.2499	0.0073
Pure error	6951.20	116.80	4	1737.80	29.20	-	-	-	-
Correlation total	67270.94	12464.94	16	-	-	-	-	-	-

### 3.3 Yield of activated carbon

The yield of activated carbon is an important parameter as it gives the amount of final product. To study the effects of the three factors on the yield of activated carbon, three-dimensional plots were drawn. The ANOVA results show that the concentration of ZnCl<sub>2</sub> ( $X_1$ ), activation time ( $X_2$ ), and the interaction terms ( $X_1X_3$ ,  $X_1^2$ , and  $X_3^2$ ) were found to have significant effects on the yield of activated carbon. Fig. 1 shows the three-dimensional surface plots for the yield of activated carbon.

Fig. 1(a) shows the combined effect of activation time and concentration of ZnCl<sub>2</sub> for the yield of activated carbon at a constant activation temperature (600 °C) and a maximum yield of 49.5% was calculated. The three-dimensional response surfaces of the most important process variables (concentration of ZnCl<sub>2</sub> and activation temperature) for the yield at a constant activation time (120 min) are shown in Fig. 1(b). ZnCl<sub>2</sub> acts as a dehydrating agent, and thus, facilitates pyrolytic decomposition and inhibits tar formation [35]. The yield of activated carbon decreased with increasing activation time and temperature; however, it increased with increasing ZnCl<sub>2</sub> concentration.

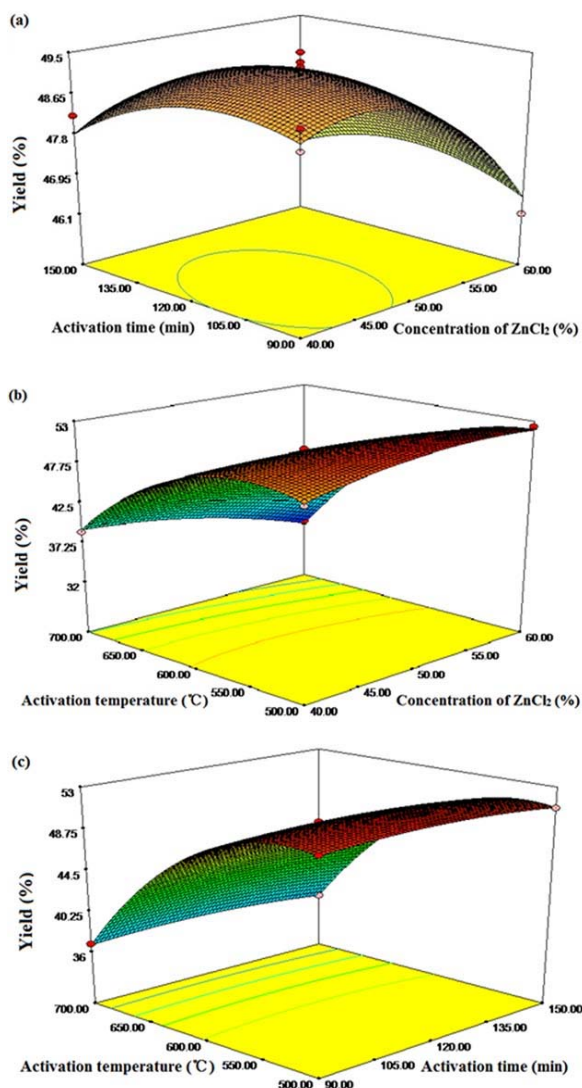


Fig. 1(a) The combined effects of activation time and concentration of ZnCl<sub>2</sub> on the yield of activated carbon at a constant activation temperature (600 °C); (b) The combined effects of activation temperature and concentration of ZnCl<sub>2</sub> on the yield of activated carbon at a constant activation time (120 min); (c) The combined effects of activation temperature and activation time on the yield of activated carbon at a constant concentration of ZnCl<sub>2</sub> (50%).

### 3.4 Adsorption of Iodine and Methylene blue

Adsorption capacity is the most important characteristics of activated carbon, and is characterized by their surface area and pore structure, which in turn are controlled by the preparation process. Three parameters selected in this study are found to have significant effect on iodine/MB adsorption. Figs. 2 and 3 show the three-dimensional response surface plots of iodine and MB adsorption, respectively.

From the ANOVA results of iodine value, three parameters were found to have insignificant effect on the

iodine adsorption value. However, activation temperature has a significant effect compared to other two factors. Fig. 2(b) shows the combined effect of activation temperature and concentration of ZnCl<sub>2</sub> for iodine value at a constant activation time (120 min). As the activation temperature increases, the iodine adsorption value also increases at first, and then decreases. This might be because more volatile compounds are released at higher temperature, which leads to open up the carbon structure resulting in more surface area. The decrease in iodine value at an activation temperature above 600 °C is probably because of the sintering effect at high temperature, followed by shrinkage of the char, and realignment of the carbon structure which resulted in reduced of surface areas.

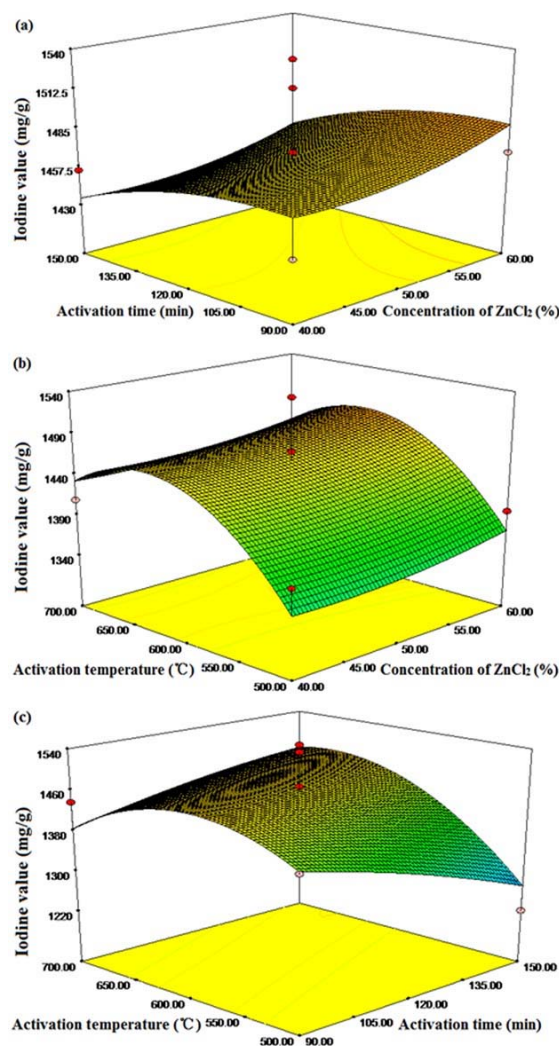


Fig. 2(a) The combined effects of activation time and concentration of ZnCl<sub>2</sub> on iodine adsorption value at a constant activation temperature (600 °C); (b) The combined effects of activation temperature and concentration of ZnCl<sub>2</sub> on iodine adsorption value at a constant activation time (120 min); (c) The combined effects of activation temperature and activation time on iodine adsorption value at a constant concentration of ZnCl<sub>2</sub> (50%).



Fig. 3 shows the three-dimensional response plots of MB adsorption. From the ANOVA results of MB value, activation temperature ( $X_3$ ) and the interaction terms ( $X_2^2$  and  $X_3^2$ ) were found to be significant, whereas the interaction terms ( $X_1^2$ ) had a very significant effect on the MB value. Fig. 3(a) shows the combined effect of activation time and concentration of  $ZnCl_2$  for the MB adsorption value at a constant activation temperature (600 °C). It shows that the MB adsorption value reaches a maximum of 300 mg/g at 600 °C. Fig. 3(b) shows the combined effect of activation temperature and concentration of  $ZnCl_2$  for the MB adsorption value at constant activation time (120 min). The MB adsorption value increases with increasing activation temperature and concentration of  $ZnCl_2$ , and then decreases. This might be due to the fact that the dehydration by  $ZnCl_2$  is aggravated and volatile compounds are released, which leads to the expansion of the pore structures. However, excessive temperature leads to ablation phenomenon of internal diameter and decrease in the MB value.

### 3.5 Process optimization

The commercial production of activated carbon requires higher product yield for economic feasibility and higher adsorption capacity for marketing advantage [30]. However, it is difficult to optimize both these responses under the same conditions because the region of interest for the process variables is difficult to achieve. As the yield of activated carbon increases, the adsorption capacity decreases and vice versa. In order to balance these three responses, the “function of desirability” was applied using a Design-Expert software version 7.1.6. The experimental conditions with the highest desirability were selected for verification using the software. The optimum conditions for preparation of activated carbon were found as follows: (i) 49.6%  $ZnCl_2$ , (ii) 112 min activation time, and (iii) 594.2 °C activation temperature, resulting in 49.6% yield, 1463.7 mg/g iodine and 292.5 mg/g MB adsorption values, as shown in Fig. 4. The experiments were repeated to verify the reliability of the predicted results obtained from the software. With regard to practical production of activated carbons, the best operating conditions were adopted as follows: 50%  $ZnCl_2$ , 120 min activation time and 600 °C activation temperature. Under these process conditions, the yield of activated carbon was 48.8% and the iodine and MB adsorption values were 1448 and 280 mg/g, respectively, which indicated the success of the process optimization exercise.

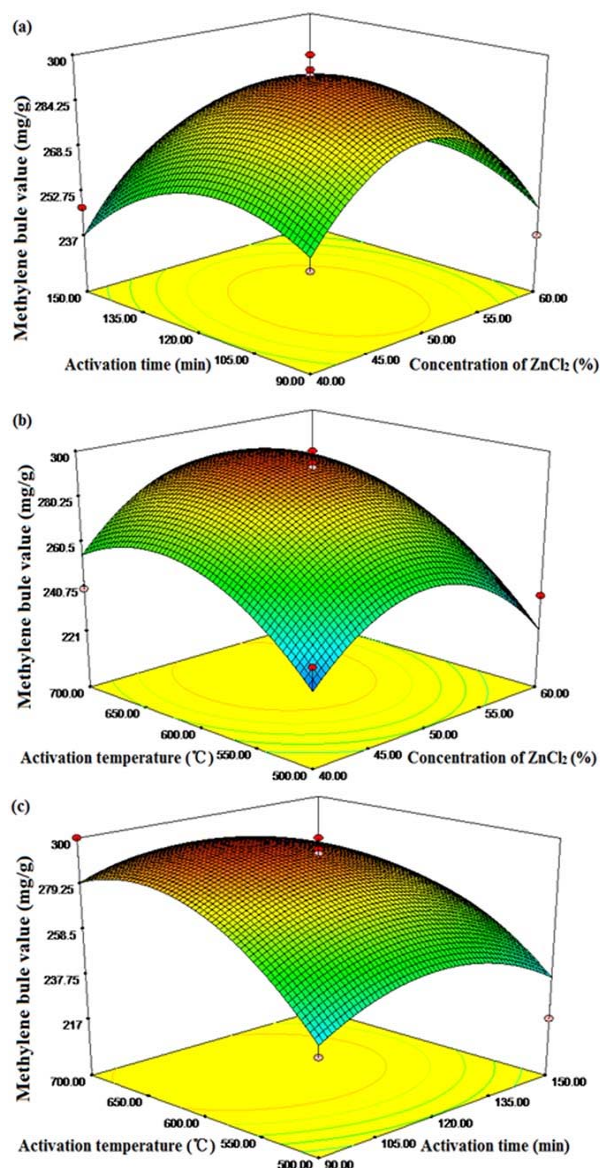


Fig. 3(a) The combined effects of activation time and concentration of  $ZnCl_2$  on methylene blue adsorption value at a constant activation temperature (600 °C); (b) The combined effects of activation temperature and concentration of  $ZnCl_2$  on methylene blue adsorption value at a constant activation time (120 min); (c) The combined effects of activation temperature and activation time on methylene blue adsorption value at a constant concentration of  $ZnCl_2$  (50%).

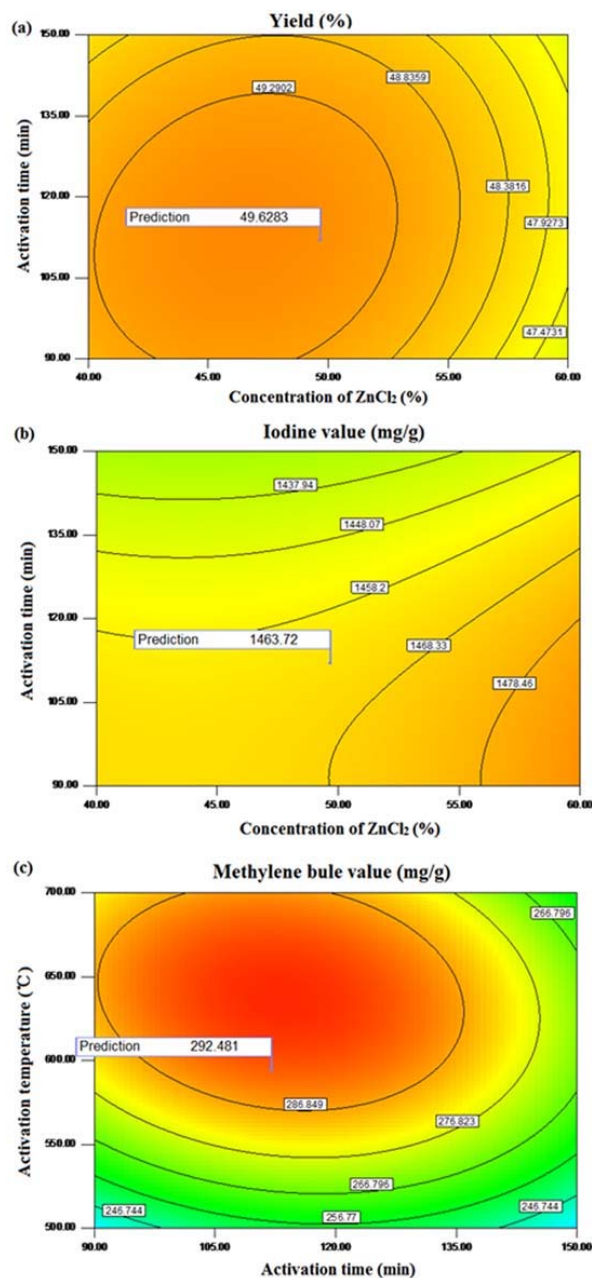


Fig. 4 Predicted optimum results of activated carbon yield (a), iodine adsorption value (b), and methylene blue adsorption value (c).

### 3.6 Characterization of activated carbon prepared under optimum conditions

The N<sub>2</sub> adsorption-desorption isotherm estimated using the automatic adsorption instrument is shown in Fig. 5. The adsorption isotherm sharply increases at low relative pressure indicating the filling of micropores and finally reaches a plateau. The adsorption capacity continues to increase with the relative pressure up to 1 atm. According to IUPAC classification, the isotherm is of

Type  $\square$ , which represents dense micropore structures. The surface area and total pore volume of the activated carbon were found to be 1449.7 m<sup>2</sup>/g and 0.8008 cm<sup>3</sup>/g, respectively, while those for *A. pedunculata* shell were 108.1 m<sup>2</sup>/g and 0.0956 cm<sup>3</sup>/g, respectively.

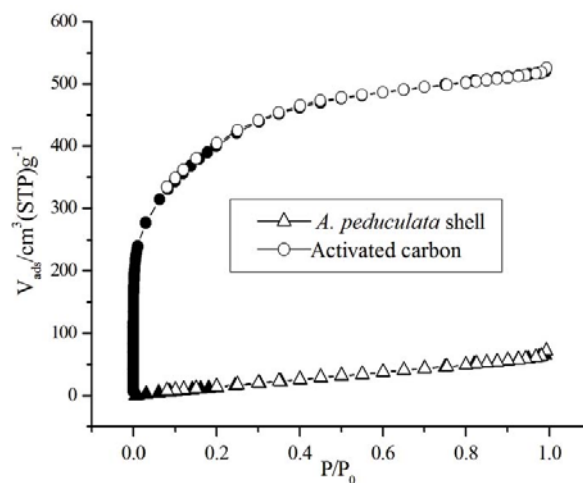


Fig. 5 N<sub>2</sub> adsorption-desorption isotherms of *A. pedunculata* shell and activated carbon.

The XRD result in Fig. 6 (a) shows the crystalline structure of the carbon layers for *A. pedunculata* shell and the prepared activated carbon. There are no significant differences in the XRD patterns for the precursor and activated carbon. This confirms that the crystalline structures of the carbon remain unchanged even after different thermal treatments. Further, broad peaks and absence of sharp peaks in the XRD pattern indicate that the activated carbons have predominantly amorphous structure, which is an advantageous for well-defined adsorbents. The broad peak observed near 24° in the XRD pattern of activated carbon indicated the presence of a crystalline carbonaceous structure with better layer alignment [36].

The FTIR spectrums shown in Fig. 6(b) present the development of surface textures in *A. pedunculata* shell and activated carbon. The IR peak around 3420 cm<sup>-1</sup> was assigned to O–H stretching vibration of hydroxyl groups. The peak at 2924 cm<sup>-1</sup> was assigned to C–H stretching vibrations of methyl groups. The Peak at 1753 cm<sup>-1</sup> was assigned to C=O stretching vibrations of esters, ketones, or aliphatic carboxylic acids. The peak at ~1045 cm<sup>-1</sup> was assigned to C–O stretching vibrations from phenolic hydroxyl groups [29], which was possibly formed due to the oxidation of the aromatic rings during the impregnation and heat treatment stages catalyzed by ZnCl<sub>2</sub> [37]. The H element and OH groups are the main components of lignocellulosic materials in *A. pedunculata* shells.



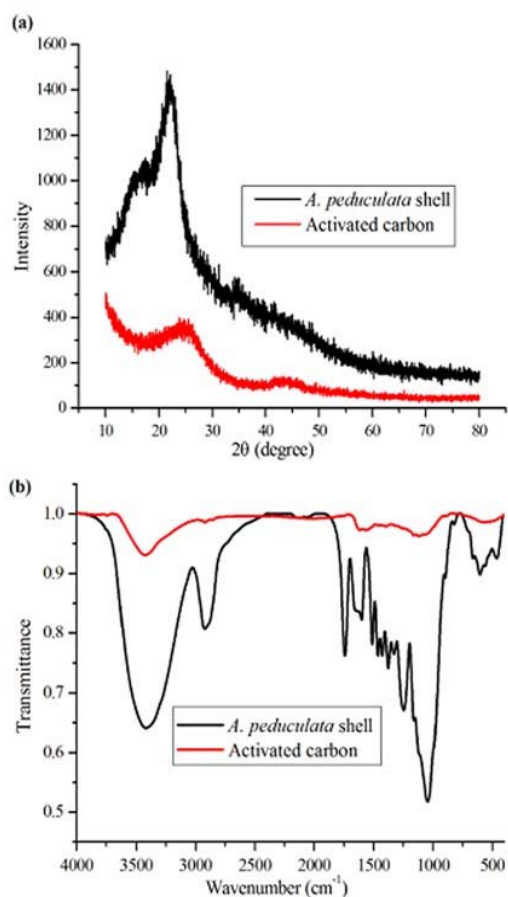


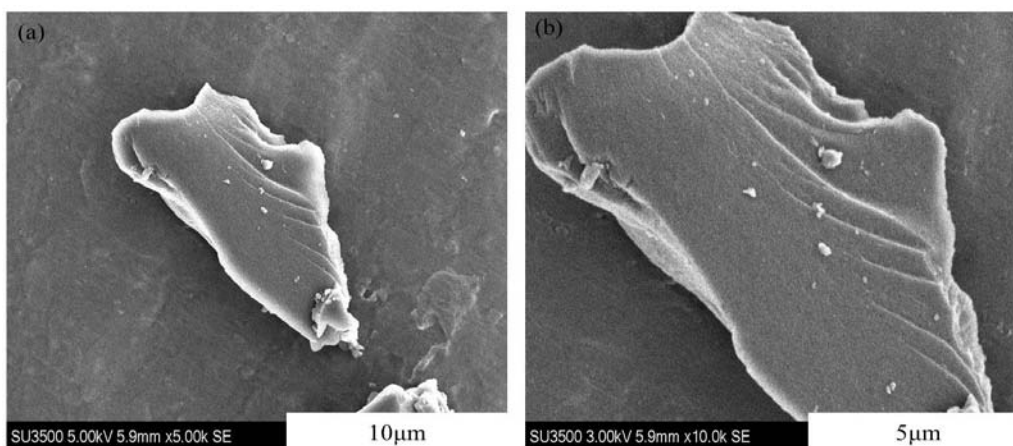
Fig. 6(a) X-ray diffraction results of *A. pedunculata* shell and activated carbon; (b) FTIR spectra of *A. pedunculata* shell and activated carbon.

#### 4. Conclusions

In this study, *Amygdalus pedunculata* shell was used to prepare activated carbon by  $\text{ZnCl}_2$  activation using Box-Behnken design. The optimum conditions for preparation of activated carbon have been identified as follows: 50%  $\text{ZnCl}_2$ , 120 min activation time, and 600 °C activation temperature leading to 48.8% yield, 1448 mg/g iodine and 280 mg/g methylene blue adsorption values. The BET surface area and pore volume of the prepared activated carbon was found to be 1449.7  $\text{m}^2/\text{g}$  and 0.8008  $\text{cm}^3/\text{g}$ , respectively. The results of this study indicate that *Amygdalus pedunculata* shells could be utilized as the feedstock for the production of high-quality activated carbons

#### Acknowledgements

This study was financially supported by Science and Technology Department of Shaanxi Province (No. 2011KTCL03-04 and No. 2012KTCL03-05) and Yulin Science technology bureau. The authors also express their gratitude to Associate Professor Xiaohui Guo and Dr. Fengchun Yang for their help.



Supplementary 1. SEM patterns of activated carbon from *A. pedunculata* shell. (a) 10  $\mu\text{m}$ ; (b) 5  $\mu\text{m}$ .

## References

- [1] R.C. Bansal, M. Goyal, Taylor & Francis Group, (2005).
- [2] N.G. Asenjo, C. Botas, C. Blanco, R. Santamaría, M. Granda, R. Menéndez, P. Alvarez, Fuel Process. Technol. **92**, 1987 (2011).
- [3] D.C.S. Azevedo, J.C.S. Araújo, M. Bastos-Neto, A.E.B. Torres, E.F. Jaguaribe, C.L. Cavalcante, Micropor. Mesopor. Mat. **100**, 361 (2007).
- [4] S. Timur, I.C. Kantarli, S. Onenc, J. Yanik, J. Anal. Appl. Pyrol. **89**, 129 (2010).
- [5] A.L. Cazetta, A.M.M. Vargas, E.M. Nogami, M.H. Kunita, M.R. Guilherme, A.C. Martins, T.L. Silva, J.C.G. Moraes, V.C. Almeida, Chem. Eng. J. **174**, 117 (2011).
- [6] O. Ioannidou, A. Zabaniotou, Sust. Energ. Rev. **11**, 1966 (2007).
- [7] P. Paraskeva, D. Kaladeris, E. Diamadopoulos, J. Chem. Technol. Biot. **83**, 581 (2008).
- [8] Y. Chen, B. Huang, M. Huang, B. Cai, J. Taiwan Inst. Chem. E. **42**, 837 (2011).
- [9] I. Kula, M. Uğurlu, H. Karaoğlu, A. Çelik, Bioresource Technol. **99**, 492 (2008).
- [10] Zhong, Q. Yang, X. Li, K. Luo, Y. Liu, G. Zeng, Ind. Crop. Prod. **37**, 178 (2012).
- [11] Ö. Şahin, C. Saka, Bioresource Technol. **136**, 163 (2013).
- [12] Y.A. Alhamed, H.S. Bamufleh, Fuel **88**, 87 (2009).
- [13] M.J. Ahmed, S.K. Theydan, Powder Technol. **229**, 237 (2012).
- [14] K.Y. Foo, B.H. Hameed, Bioresource Technol. **111**, 425 (2012).
- [15] J. Chu, X. Xu, Y. Zhang, Bioresource Technol. **134**, 374 (2013).
- [16] Y. Shen, C. Li, Y. Zhang, B. Li, Y. Fan, Northwest University CN101731367A (2010).
- [17] Y. Shen, C. Li, Y. Zhang, B. Li, Y. Fan, Northwest University CN101723361A (2010).
- [18] K. Fu, Q. Yue, B. Gao, Y. Sun, L. Zhu, Chem. Eng. J. **228**, 1074 (2013).
- [19] S. Guo, J. Peng, W. Li, K. Yang, L. Zhang, S. Zhang, H. Xia, Appl. Surf. Sci. **163**, 8443 (2009).
- [20] N.V. Sych, S.I. Trofymenko, O.I. Poddubnaya, M.M. Tsyba, V.I. Sapsay, D.O. Klymchuk, A.M. Puziy, Appl. Surf. Sci. **261**, 75 (2012).
- [21] R.L. Tseng, S.K. Tseng, J. Colloid Interf. Sci. **287**, 428 (2005).
- [22] H. Deng, G. Li, H. Yang, J. Tang, J. Tang, Chem. Eng. J. **163**, 373 (2010).
- [23] J. Yang, K. Qiu, Chem. Eng. J. **165**, 209 (2010).
- [24] I.I. Gurten, M. Ozmak, E. Yagmur, Z. Aktas, Biomass Bioenergy **37**, 73 (2012).
- [25] M. Al Bahri, L. Calvo, M.A. Gilarranz, J.J. Rodriguez, Chem. Eng. J. **203**, 348 (2012).
- [26] A. Elmouwahidi, Z. Zapata-Benabithé, F. Carrasco-Marín, C. Moreno-Castilla, Bioresource Technol. **111**, 185 (2012).
- [27] G. Moussavi, A. Alahabadi, K. Yaghmaeian, M. Eskandari, Chem. Eng. J. **217**, 119 (2013).
- [28] F. Karacan, U. Ozden, S. Karacan, Appl. Therm. Eng. **27**, 1212 (2007).
- [29] J. N. Sahu, J. Acharya, B.C. Meikap, Bioresource Technol. **101**, 1974 (2010).
- [30] S.K. Theydan, M.J. Ahmed, Power Technol. **224**, 101 (2012).
- [31] G.E.P. Box, D.W. Behnken, Technometrics **2**, 455 (1960).
- [32] A. Kumar, B. Prasad, I.M. Mishra, J. Hazard Mater. **150**, 174 (2008).
- [33] X. Duan, C. Srinivasakannan, J. Peng, L. Zhang, Z. Zhang, Fuel Process. Technol. **92**, 394 (2011).
- [34] H. Deng, L. Yang, G. Tao, J. Dai, J. Hazard Mater. **166**, 1514 (2009).
- [35] C. Saka, BET, TG, FT-IR, SEM, J. Anal. Appl. Pyrol. **95**, 21 (2012).
- [36] W. Tongpoothorn, M. Sriuttha, P. Homchan, S. Chanthai, C. Ruangviriyachai, Chem. Eng. Res. Des. **89**, 334 (2011).
- [37] S. Uçar, M. Erdem, T. Tay, S. Karagöz, Appl. Surf. Sci. **225**, 8890 (2009).